

An enhanced macroscopic inverse flexoelectric-like response in flexoelectrets

X. Wen¹, K. Tan¹, Q. Deng^{1*}, S. Shen^{1*}.

Affiliations: ¹State Key Laboratory for Strength and Vibration of Mechanical Structures, School of Aerospace Engineering, Xi'an Jiaotong University, Xi'an 710049, China.

***Corresponding author:** tonydqian@mail.xjtu.edu.cn (Q.D.); sshen@mail.xjtu.edu.cn (S.S.)

Abstract:

Flexoelectricity allows a dielectric material to bend in response to a uniform electric field, and adds a new degree of freedom for designing actuators. However, its applications are usually limited to the nanoscale due to its inherent size effect. Here, we report an enhanced macroscopic flexoelectric-like response in flexoelectrets (soft elastomers with embedded charges), showing excellent actuation performance comparable with nanoscale flexoelectric actuators. Theoretical analysis indicates that the symmetry breaking of Maxwell stress is the cause of this enhancement. This work opens an avenue for applying macroscopic flexoelectricity in actuators and flexible electronics.

Main text:

Usually, a uniform electric field can cause a single electro-active material which is homogeneous and isotropic deform uniformly via electromechanical couplings such as piezoelectricity [1], electrostriction [2], and Maxwell stress effect [3], which is widely used in actuations such as robotics [4, 5] and artificial muscles [6]. To bend such homogeneous and isotropic active materials, a common way is to apply asymmetric constraints to it. For example, attaching a piece of active material onto the upper or lower surface of a passive cantilever beam which doesn't response to the applied electric field can convert the uniform deformation into bending. This idea of generating bending indirectly has been intensively applied in all kinds of actuators for decades [4-7] due to the advantages of bending deformation [8, 9]. However, how to couple a uniform electric field with curvature directly remains a challenging problem.

A good candidate may be flexoelectricity, a universal and direct coupling between strain gradient (such as bending) and polarization in dielectrics [10-12]. Flexoelectricity is a two-way electromechanical coupling. In the past decade, direct flexoelectricity (polarization induced by

strain gradient) has shown its great potential in applications including information storage and reading [13-15], tuning electronic properties [16-19], flexible electronics [20], bone repairing [21], energy harvesting [22, 23], etc. On the other hand, converse (uniform strain induced by the gradient of electric field) and inverse (curvature induced by uniform electric field) flexoelectricity, although still in their infancy [10], were reported both theoretically [24-26] and experimentally [27-33]. Like the direct flexoelectric effect, an inverse flexoelectric effect also shows strong size dependence [21, 31, 34-37]. Bursian et al. proposed that, because of the inverse flexoelectric effect, the induced curvature κ of a dielectric cantilever beam was related to the uniformly applied electric field E_V by [10]

$$\kappa = 12(1 - \nu^2) \frac{\mu_{12} E_V}{Y h^2}, \quad (1)$$

where μ_{12} is the transverse flexoelectric coefficient, ν denotes Poisson's ratio, Y is Young's modulus, and h is the thickness of the beam. With the decrease of h , the induced curvature κ increases fast for a fixed applied electric field. Thus, as shown in Fig. 1(a), inverse flexoelectricity reduces sharply with the increase of the sample's feature size. The size effect seems to be an inevitable constraint to the application of both direct and inverse flexoelectricity at the macroscale. Although several recent works show that the bending-induced polarization can be enhanced by 1~3 orders of magnitude through introducing the so-called flexoelectric-like response [38-41], there is no evidence that these extrinsic mechanisms can naturally lead to an enhanced inverse response. For the barrier-layer-mechanism, the most famous one among the above mechanisms, the electric-field-induced bending may be even weaker than its counterpart of intrinsic flexoelectricity [38].

In this letter, we aim to explore a way to break the constraint and introduce the inverse flexoelectric effect to macroscopic applications. Recently, we reported an enhanced flexoelectric-like response (bending-induced polarization) in flexoelectrets [41], of which a charge layer was embedded in silicone rubber. By this enhanced flexoelectric-like response, at the macroscale, the effective flexoelectricity of silicone rubber was increased by two orders in magnitude. Large coefficient and small Young's modulus in flexoelectrets provide a good opportunity to investigate the corresponding inverse phenomenon according to equation (1). As we will see in this letter, this electromechanical response is a two-way coupling, which allows flexoelectrets to bend in response to an external electric field. The basic mechanism underpinning the inverse

phenomenon, the macroscopic symmetry breaking of Maxwell stress, is illustrated in Fig. 1(b) and (c): one layer of negative charge is embedded in an elastomer beam, resulting in a pre-existing electric field (red arrows) which is symmetric about the charged plane. When a uniform external electric field (yellow arrows) is applied, they superpose throughout the sample and results in larger electric field in the upper part while smaller electric field in the lower part. Hence, a macroscopic symmetry breaking of stretching in the sample, induced by Maxwell stress effect, is expected and leads to curvature eventually. This bending deformation would be further amplified due to the small Young's modulus of the material (56.79KPa).

To demonstrate our idea, we fabricated flexoelectrets by embedding a charged thin film in the middle plane of an elastomer cantilever (see Supplemental Material [42] for material fabrication). Fig. 2(a) illustrates a brief schematic experimental setup: a laser displacement sensor was used to detect the displacement of the cantilever end generated by sinusoidal voltage from a high voltage supply (see Supplemental Material [42] for experimental setup). Since the elastomer is non-polar, piezoelectricity is excluded here to explain any possible deformations induced by voltage (see Supplemental Material [42] for material characterization).

Flexoelectret embedded a charge layer with a density of -0.088mC/m^2 was stimulated by a sinusoidal voltage (1Hz) with a peak of 1kV. The red solid line in Fig. 2(b) shows the induced Fourier-filtered first-harmonic displacement (see Supplemental Material [42] for unfiltered data). Moreover, this pronounced curvature (calculated from the P-P value of the Fourier-filtered displacement) varies linearly with the applied electric field (Fig. 2(c)). These responses of flexoelectrets show typical inverse flexoelectric characteristics, which is the first time that flexoelectric bending was observed at the macroscale. To exam how much the intrinsic inverse flexoelectricity contributes to the bending of the cantilever, a similar elastomer cantilever but without charged layer was set to be a control group and tested at the same voltage stimulation. As shown by the red dashed line in Fig. 2(b), without the charged layer, no first-harmonic oscillations were observed, which experimentally verified the fact that the intrinsic flexoelectricity is too weak to be observed at the macroscale as we mentioned above. Therefore, the bending deformations observed here originate from the charge layer in flexoelectrets rather than the distortion of material's microstructures (intrinsic mechanism) [27], termed here as inverse flexoelectric-like response. According to equation (1), the effective flexoelectric

coefficient of flexoelectrets (-0.088mC/m^2) was obtained: $\mu_{12}^{eff} = 10.3\text{nC/m}$, comparable to the most famous flexoelectric polymer polyvinylidene difluoride (PVDF) [43]. Note that the flexoelectret introduced here is much softer than PVDF (Young's modulus is more than 4 orders of magnitude smaller), which results in much larger bending deformation than that of PVDF according to equation (1).

To further confirm the effect of the charge layer on this enhancement of inverse flexoelectricity, we changed the polarity of the charge layer (0.086mC/m^2). Fig. 2(d) shows that the bending direction was reversed under the same voltage stimulation in Fig. 2(b). We further changed the magnitude of the charge density and found that the induced curvature increases almost linearly with the charge density (Fig. 2(e)). These observations provide strong evidence that the enhanced flexoelectric-like in flexoelectrets should be attributed to the embedded charge layer and it is tunable via manipulating the charge layer. Nevertheless, how the charge layer influences the electromechanical coupling is still not clear.

To identify the main cause of the enhanced flexoelectric phenomenon, in this work, we establish an electrostatic model (Fig. 3(a)) in which the only electromechanical coupling mechanism is the Maxwell stress effect. The distribution of electric field can be calculated from Gauss' law, which comes from external voltage (yellow arrows) and the charge layer (red arrows). When no voltage is applied to the model, the charge layer generates an electric field with the same magnitude but opposite direction across the model (Fig. 3(b)), leading to uniform Maxwell stress (Fig. 3(c)). At the excitation of the voltage, the symmetric state of stress was broken. Specifically, one part experienced larger stretching stress than the other part, which can be expressed as (see Supplemental Material [42] for detailed derivations)

$$p_2^a = \frac{1}{2} \varepsilon \left(\frac{q}{2\varepsilon} - E_V \right)^2 \quad (2)$$

and

$$p_2^b = \frac{1}{2} \varepsilon \left(\frac{q}{2\varepsilon} + E_V \right)^2, \quad (3)$$

where ε is permittivity, q is the density of the charge layer, p_2^a and p_2^b denote the Maxwell stress p_2 (along x_2 direction) above and below the charge layer respectively. Equation (2) and (3) shows the typical nonlinear characteristic of Maxwell stress [6, 44]. Such distributions of stress

are equivalent to a resultant force F plus a bending moment M (Fig. 3(c)), which can be obtained as

$$F = b \int_{-\frac{h}{2}}^{\frac{h}{2}} p_2 dx_1 = \frac{bhq^2}{8\varepsilon} + \frac{\varepsilon bhE_v^2}{2} \quad (4)$$

and

$$M = b \int_{-h/2}^{h/2} x_1 p_2 dx_1 = -\frac{qbE_v h^2}{8} \quad (5)$$

Interestingly, in the above two equations, the square term of the applied electric field E_v^2 remains in the former one but is eliminated in the latter one, which implies a linear coupling between curvature κ and external electric field E_v that can be obtained as

$$\kappa = \frac{M}{YI} = -\frac{3}{2} \frac{qE_v}{Yh}, \quad (6)$$

where $I = bh^3/12$ is the bending stiffness which links the bending moment to the induced curvature of a beam. This formula predicts that the bending direction depends on the polarity of the charge density and applied voltage, consistent with our experimental observations. We also performed finite element (FEM) calculations considering Maxwell stress effect to solve this problem (see Supplemental Material [42] for FEM calculations). As shown in Fig. 3(d) and (e), our theoretical and simulation results show good agreements with experimental results for samples with different charge densities or thickness. Thus, the origin of the inverse flexoelectric-like response can be understood: the charge layer introduces a macroscopic symmetry breaking of Maxwell stress, which transforms nonlinear Maxwell stress effect into a linear flexoelectric-like response.

In Fig. 4(a), the actuation performance evaluated by curvature/electric field ratio for our flexoelectrets and typical flexoelectrics like SiTiO₃ [29, 31] and BaTiO₃ [27] are compared. It can be seen that flexoelectrets become the first flexoelectric member that shows enhanced inverse flexoelectricity at the macroscale, which is not only due to the soft materials it composed of, but, more importantly, also because of the nature of the flexoelectric-like effect itself. For intrinsic inverse flexoelectric effect, as shown by equation (1), the induced curvature is proportional to $1/h^2$. However, for the flexoelectric-like effect introduced here, as shown by equation (6), the induced curvature is proportional to $1/h$. This difference results in quite different size dependency of them, which is schematically plotted in Fig. 4(b). Under a fixed

external electric field, the bending angle of a traditional flexoelectric beam decreases fast with the increase of the sample size. While for the flexoelectret showing flexoelectric-like behaviors, the bending angle of the beam is independent of the sample size. In other words, the induced displacement of the flexoelectret scales up with the increase of sample size. Thus, the flexoelectric-like effect we introduced here breaks the constraint of size effect that limits the applications of flexoelectricity to the nanoscale.

In summary, this work demonstrates that size growth does not necessarily result in deterioration of inverse flexoelectricity. Our flexoelectrets show enhanced macroscopic inverse flexoelectric-like response, which originates from the macroscopic symmetry breaking of Maxwell stress. Because of the universality of Maxwell stress effect, this effective flexoelectricity is universal in all dielectrics and particularly significant in soft materials. Given that curvature and electric field are coupled directly here, our work provides a new degree of freedom for designing actuators and flexible electronics, which is helpful to simplify device design, avoid interface failure and achieve novel functional properties that are previously inaccessible. More generally, in flexoelectrets, both direct [41] and inverse (this work) flexoelectricity are set free from size effect and then extended to the macroscale, providing a fertile ground for exploring novel flexoelectric applications. Additionally, flexoelectrets can also serve as a platform in which flexoelectricity can be coupled to other functional properties such as ferroelectricity [13] and magnetism [45, 46], since these properties are easily introduced to silicone elastomer/rubber [47, 48].

Acknowledgments:

We gratefully acknowledge the support from the National Key R&D Program of China (2017YFE0119800), the National Natural Science Foundation of China (Grant Nos. 11632014, 11672222, and 11372238), the 111 Project (B18040), the Chang Jiang Scholar Program, and numerous helpful discussions with J. Liu (Xi'an Jiaotong University).

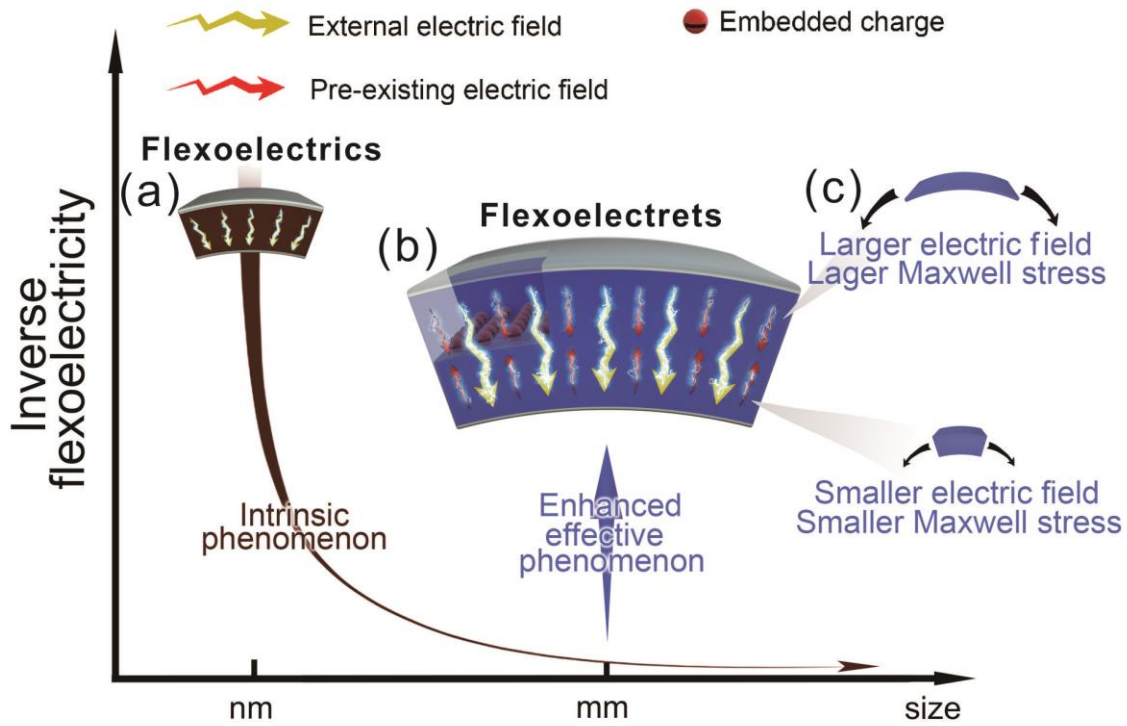


FIG. 1. Schematic illustration of the mechanism of effective inverse flexoelectricity in flexoelectrets. (a) An external electric field (yellow arrows) is capable of bending a dielectric material via intrinsic flexoelectricity, which is significant at the nanoscale while decreases dramatically with size increases. **(b)** The enhanced effective flexoelectricity in flexoelectrets that have a layer of embedded negative charge (red spheres) and consequent pre-existing electric field (red arrows). Above the charge layer, pre-existing and external electric field have the same direction and add to each other. Below the charge layer, situations are the opposite. **(c)** Thus, upper and lower parts undergo different true electric field and consequent different stretching stress via Maxwell stress effect, leading to bending deformation.

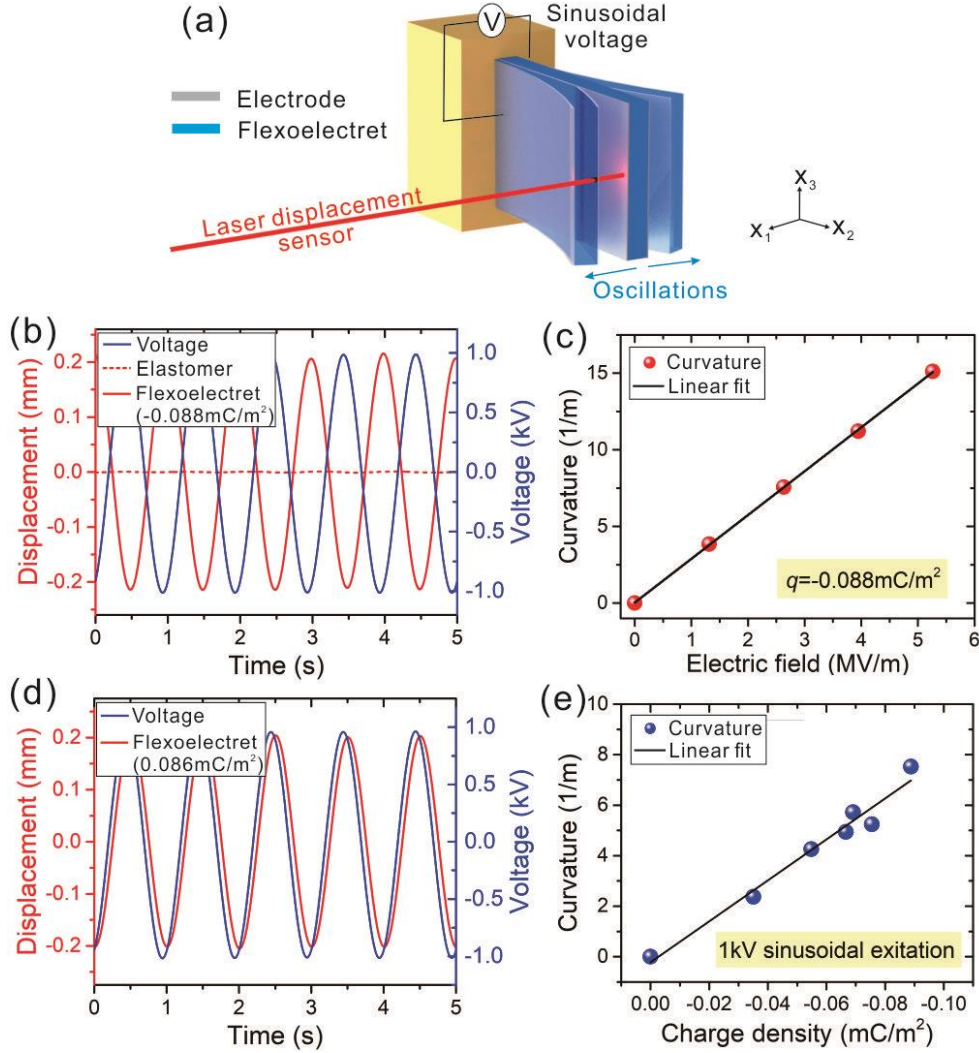


FIG. 2. Experimental setup and results. (a) Experimental setup consisting of a clamping rigid body, a high voltage supply, and a laser displacement sensor. (b) Applied voltage (blue solid line) and induced first-harmonic displacement of cantilever end. Red dashed line and red solid line represent elastomer without charge and flexoelectret with a charge density of -0.088 mC/m^2 , respectively. (c) Curvature as a function of the applied electric field for flexoelectret (-0.088 mC/m^2). (d) Applied voltage (blue solid line) and induced first-harmonic displacement of flexoelectrets cantilever end. The charge density of the middle layer is positive (0.086 mC/m^2). (e) Curvature as a function of the magnitude of charge density for flexoelectrets with the bias of 1kV. All results in this figure were acquired for the sample with a size of $10 \text{ mm} \times 7 \text{ mm} \times 0.76 \text{ mm}$ at sinusoidal excitation of 1Hz at room temperature.

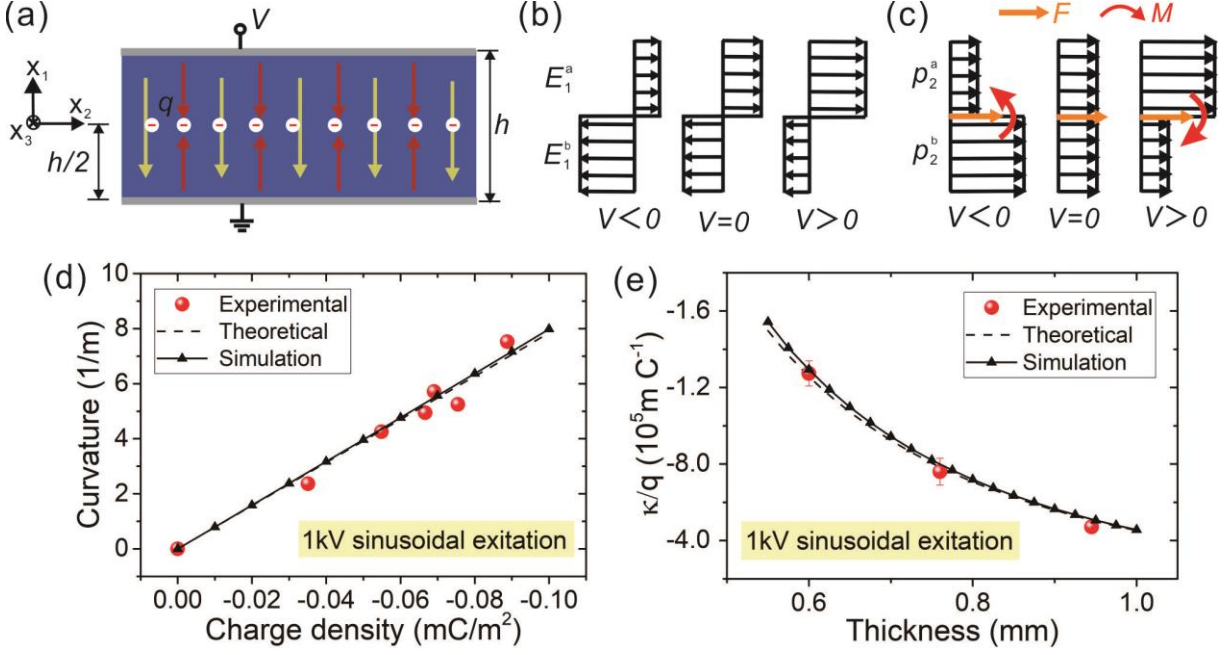


FIG. 3. Electrostatic model of a flexoelectret and comparison between experimental, theoretical and simulation results. (a) Theoretical model of a flexoelectret. The white circles represent the charge layer. The red and yellow arrows represent the electric field from the charge layer and external voltage respectively. (b and c) Distribution of electric field E_1 (b) and Maxwell stress p_2 (c) in cross-section. The stress is equivalent to a resultant force F ($V=0$) or a resultant force F plus a bending moment M ($V \neq 0$). (d and e) Curvature as a function of charge density (d) and thickness (e) and the comparison of experimental, theoretical, and simulation results. To only investigate the influence from thickness change, we divide the curvature κ by charge q because it is difficult to control charge density accurately.

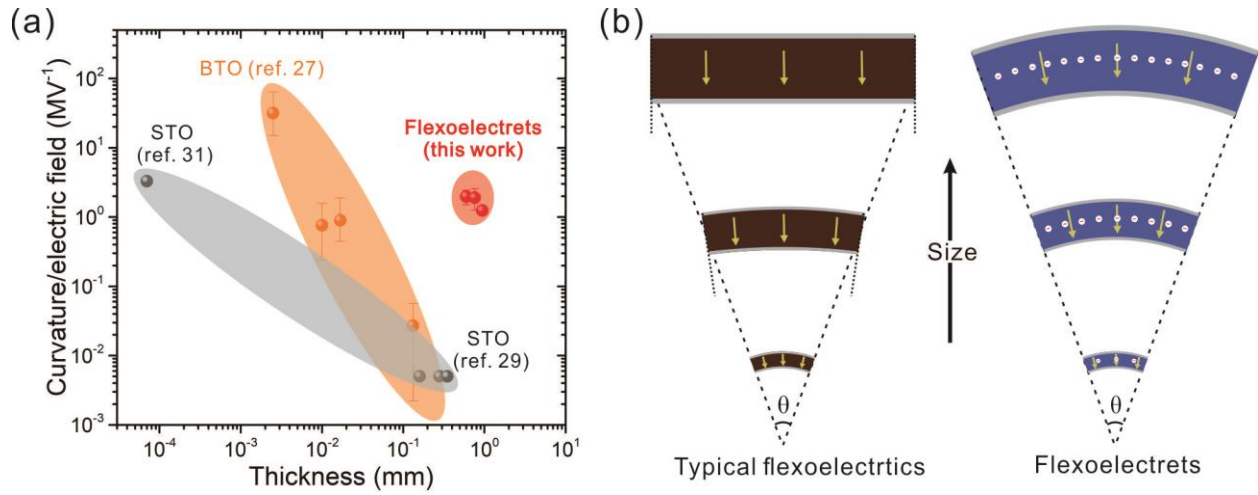


FIG. 4. Comparison of the performance of flexoelectrets with typical flexoelectrics. (a) The ratios of curvature/electric field as a function of thickness are compared for flexoelectrets (this work) and flexoelectric SiTiO_3 [29, 31] and BaTiO_3 [27]. (b) The evolution of bending performance under a fixed applied electric field (yellow arrows) when the size is scaled up.

References and Notes:

- [1] S.-E. Park, T. R. ShROUT, Ultrahigh strain and piezoelectric behavior in relaxor based ferroelectric single crystals. *J Appl Phys* **82**, 1804-1811 (1997).
- [2] W. Lehmann, H. Skupin, C. Tolksdorf, E. Gebhard, R. Zentel, P. Kruger, M. Losche, F. Kremer, Giant lateral electrostriction in ferroelectric liquid-crystalline elastomers. *Nature* **410**, 447-450 (2001).
- [3] R. Pelrine, R. Kornbluh, Q. Pei, J. Joseph, High-speed electrically actuated elastomers with strain greater than 100%. *Science* **287**, 836-839 (2000).
- [4] Y. Wu *et al.*, Insect-scale fast moving and ultrarobust soft robot. *Science Robotics* **4**, eaax1594 (2019).
- [5] T. Li *et al.*, Fast-moving soft electronic fish. *Sci Adv* **3**, e1602045 (2017).
- [6] E. Acome, S. K. Mitchell, T. G. Morrissey, M. B. Emmett, C. Benjamin, M. King, M. Radakovitz, C. Keplinger, Hydraulically amplified self-healing electrostatic actuators with muscle-like performance. *Science* **359**, 61-65 (2018).
- [7] J. H. Yoo, J. I. Hong, W. Cao, Piezoelectric ceramic bimorph coupled to thin metal plate as cooling fan for electronic devices. *Sensors and Actuators A: Physical* **79**, 8-12 (2000).
- [8] A. Erturk, D. J. Inman, An experimentally validated bimorph cantilever model for piezoelectric energy harvesting from base excitations. *Smart Mater Struct* **18**, 025009 (2009).
- [9] A. H. Rahmati, S. Yang, S. Bauer, P. Sharma, Nonlinear bending deformation of soft electrets and prospects for engineering flexoelectricity and transverse (d31) piezoelectricity. *Soft Matter* **15**, 127-148 (2018).
- [10] P. Zubko, G. Catalan, A. K. Tagantsev, Flexoelectric Effect in Solids. *Annual Review of Materials Research* **43**, 387-421 (2013).
- [11] B. Wang, Y. Gu, S. Zhang, L.-Q. Chen, Flexoelectricity in solids: Progress, challenges, and perspectives. *Progress in Materials Science*, 100570 (2019).
- [12] P. Zubko, G. Catalan, A. Buckley, P. R. Welche, J. F. Scott, Strain-gradient-induced polarization in SrTiO₃ single crystals. *Phys Rev Lett* **99**, 167601 (2007).
- [13] H. Lu, C. W. Bark, D. Esque de los Ojos, J. Alcala, C. B. Eom, G. Catalan, A. Gruverman, Mechanical writing of ferroelectric polarization. *Science* **336**, 59-61 (2012).

- [14] K. Cordero-Edwards, N. Domingo, A. Abdollahi, J. Sort, G. Catalan, Ferroelectrics as Smart Mechanical Materials. *Advanced Materials* **29**, (2017).
- [15] S. M. Park, B. Wang, S. Das, S. C. Chae, J. S. Chung, J. G. Yoon, L. Q. Chen, S. M. Yang, T. W. Noh, Selective control of multiple ferroelectric switching pathways using a trailing flexoelectric field. *Nat Nanotechnol*, (2018).
- [16] D. Lee, S. M. Yang, J. G. Yoon, T. W. Noh, Flexoelectric rectification of charge transport in strain-graded dielectrics. *Nano Lett* **12**, 6436-6440 (2012).
- [17] P. Sharma *et al.*, Mechanical Tuning of LaAlO₃/SrTiO₃ Interface Conductivity. *Nano Lett* **15**, 3547-3551 (2015).
- [18] F. Zhang *et al.*, Modulating the Electrical Transport in the Two-Dimensional Electron Gas at LaAlO₃/SrTiO₃ Heterostructures by Interfacial Flexoelectricity. *Phys Rev Lett* **122**, 257601 (2019).
- [19] L. McGilly *et al.*, Seeing moiré superlattices. *arXiv preprint arXiv:1912.06629*, (2019).
- [20] G. Dong *et al.*, Super-elastic ferroelectric single-crystal membrane with continuous electric dipole rotation. *Science* **366**, 475-479 (2019).
- [21] F. Vazquez-Sancho, A. Abdollahi, D. Damjanovic, G. Catalan, Flexoelectricity in Bones. *Adv Mater* **30**, (2018).
- [22] B. Wang, S. Yang, P. Sharma, Flexoelectricity as a universal mechanism for energy harvesting from crumpling of thin sheets. *Physical Review B* **100**, (2019).
- [23] Q. Deng, M. Kammoun, A. Erturk, P. Sharma, Nanoscale flexoelectric energy harvesting. *International Journal of Solids and Structures* **51**, 3218-3225 (2014).
- [24] E. V. Bursian, N. N. Trunov, Nonlocal piezoelectric effect. *Sov. Phys. Solid State* **16**, 760–762 (1974).
- [25] L. Shu, F. Li, W. Huang, X. Wei, X. Yao, X. Jiang, Relationship between direct and converse flexoelectric coefficients. *J Appl Phys* **116**, 144105 (2014).
- [26] A. Abdollahi, C. Peco, D. Millán, M. Arroyo, I. Arias, Computational evaluation of the flexoelectric effect in dielectric solids. *J Appl Phys* **116**, 093502 (2014).
- [27] E. V. Bursian, O. I. Zaikovskii, Changes in curvature of ferroelectric film due to polarization. *Sov. Phys. Solid State* **10**, 1121-1124 (1968).

- [28] J. Y. Fu, W. Zhu, N. Li, L. E. Cross, Experimental studies of the converse flexoelectric effect induced by inhomogeneous electric field in a barium strontium titanate composition. *J Appl Phys* **100**, 024112 (2006).
- [29] V. G. Zalesskii, E. D. Rumyantseva, Converse flexoelectric effect in the SrTiO₃ single crystal. *Physics of the Solid State* **56**, 1352-1354 (2014).
- [30] L. Shu, W. Huang, S. Ryung Kwon, Z. Wang, F. Li, X. Wei, S. Zhang, M. Lanagan, X. Yao, X. Jiang, Converse flexoelectric coefficient f_{1212} in bulk Ba_{0.67}Sr_{0.33}TiO₃. *Appl Phys Lett* **104**, 232902 (2014).
- [31] U. K. Bhaskar, N. Banerjee, A. Abdollahi, Z. Wang, D. G. Schlom, G. Rijnders, G. Catalan, A flexoelectric microelectromechanical system on silicon. *Nat Nanotechnol* **11**, 263-266 (2016).
- [32] P. Koirala, C. A. Mizzi, L. D. Marks, Direct Observation of Large Flexoelectric Bending at the Nanoscale in Lanthanide Scandates. *Nano Lett* **18**, 3850-3856 (2018).
- [33] A. Abdollahi, N. Domingo, I. Arias, G. Catalan, Converse flexoelectricity yields large piezoresponse force microscopy signals in non-piezoelectric materials. *Nat Commun* **10**, 1266 (2019).
- [34] D. Lee, A. Yoon, S. Y. Jang, J. G. Yoon, J. S. Chung, M. Kim, J. F. Scott, T. W. Noh, Giant flexoelectric effect in ferroelectric epitaxial thin films. *Phys Rev Lett* **107**, 057602 (2011).
- [35] C. A. Mizzi, A. Y. W. Lin, L. D. Marks, Does Flexoelectricity Drive Triboelectricity? *Phys Rev Lett* **123**, 116103 (2019).
- [36] K. Cordero-Edwards, H. Kianirad, C. Canalias, J. Sort, G. Catalan, Flexoelectric Fracture-Ratchet Effect in Ferroelectrics. *Phys Rev Lett* **122**, 135502 (2019).
- [37] P. Gao, S. Yang, R. Ishikawa, N. Li, B. Feng, A. Kumamoto, N. Shibata, P. Yu, Y. Ikuhara, Atomic-Scale Measurement of Flexoelectric Polarization at SrTiO₃ Dislocations. *Phys Rev Lett* **120**, 267601 (2018).
- [38] J. Narvaez, F. Vasquez-Sancho, G. Catalan, Enhanced flexoelectric-like response in oxide semiconductors. *Nature* **538**, 219-221 (2016).
- [39] A. Abdollahi, F. Vasquez-Sancho, G. Catalan, Piezoelectric Mimicry of Flexoelectricity. *Phys Rev Lett* **121**, 205502 (2018).
- [40] X. Zhang, Q. Pan, D. Tian, W. Zhou, P. Chen, H. Zhang, B. Chu, Large Flexoelectriclike

- Response from the Spontaneously Polarized Surfaces in Ferroelectric Ceramics. *Phys Rev Lett* **121**, 057602 (2018).
- [41] X. Wen, D. Li, K. Tan, Q. Deng, S. Shen, Flexoelectret: An Electret with a Tunable Flexoelectriclike Response. *Phys Rev Lett* **122**, 148001 (2019).
- [42] See Supplemental Material for material fabrication and characterization, experimental setup, unfiltered displacement data, derivation of the inverse flexoelectric-like response, and FEM calculations,.
- [43] B. Chu, D. R. Salem, Flexoelectricity in several thermoplastic and thermosetting polymers. *Appl Phys Lett* **101**, 103905 (2012).
- [44] C. Keplinger, J. Y. Sun, C. C. Foo, P. Rothmund, G. M. Whitesides, Z. Suo, Stretchable, transparent, ionic conductors. *Science* **341**, 984-987 (2013).
- [45] E. A. Eliseev, A. N. Morozovska, M. D. Glinchuk, R. Blinc, Spontaneous flexoelectric/flexomagnetic effect in nanoferroics. *Physical Review B* **79**, (2009).
- [46] E. A. Eliseev, M. D. Glinchuk, V. Khist, V. V. Skorokhod, R. Blinc, A. N. Morozovska, Linear magnetoelectric coupling and ferroelectricity induced by the flexomagnetic effect in ferroics. *Physical Review B* **84**, (2011).
- [47] W. Hu, G. Z. Lum, M. Mastrangeli, M. Sitti, Small-scale soft-bodied robot with multimodal locomotion. *Nature* **554**, 81-85 (2018).
- [48] G. Zhang, P. Zhao, X. Zhang, K. Han, T. Zhao, Y. Zhang, C. Jeong, S. Jiang, S. Zhang, Q. Wang, Flexible three-dimensional interconnected piezoelectric ceramic foam based composites for highly efficient concurrent mechanical and thermal energy harvesting. *Energy & Environmental Science* **11**, 2046-2056 (2018).